

Development of a Lorentz-force Actuated Intravitreal Jet Injector*

James E. White¹, Jean H. Chang², N. Catherine Hogan³, and Ian W. Hunter⁴

Abstract—Intravitreal injection is a common treatment in ophthalmology, but it can lead to numerous complications. Needle-free jet injection has been shown to successfully deliver fluid to various layers of skin, and, by its nature, may reduce intravitreal injection complications. From injection trials into *ex vivo* rabbit eyes, we find that needle-free jet injection can be used for intravitreal drug delivery. A custom-designed control scheme, characterized in this study, is crucial to this delivery. The system is capable of delivering 40 μL of fluid to the posterior vitreous humor, with an injection duration less than 100 ms and scleral entry site less than 350 μm in diameter.

I. INTRODUCTION

Intravitreal (IV) injection is a necessary procedure for treatment of eye diseases such as age-related macular degeneration [1], proliferative diabetic retinopathy [2], and endophthalmitis [3]. The procedure demands constant focus and dexterity from an ophthalmologist. Mistakes are uncommon but can lead to serious complications [4] such as lens damage, retinal damage, and infection. Repeated injections are often required over extended periods, and while patient compliance leads to better visual health, discomfort and anxiety may cause reduced compliance [5].

Lorentz-force actuated needle-free jet injection (JI) technology developed at the MIT BioInstrumentation Lab [6] was identified as a promising solution to the complications and anxiety introduced with needle IV injection. In an earlier injector device, voltage is set across a voice coil which slides along a fixed magnet. A real-time control and data acquisition system actively monitors and servo-controls the position of the coil, which is specified by a pre-set waveform. The coil is attached to a syringe which ejects drug through a small nozzle at high speeds. The nozzle is placed in contact with tissue and an injection is initiated with a button.

This technology was adapted to IV injections for a number of reasons. Injection depth can be controlled into several tissue types by changing the pre-set waveform parameters [7], and it was hypothesized that this would hold true for the eye. The absence of a needle anywhere inside the orbit

prevents accidental stick wounds and decreases the risk of endophthalmitis. Injections are performed much more quickly, reducing patient anxiety and increasing compliance.

Previous work includes the development of a hybrid microneedle-jet injector [8]. A microneedle (412.8 μm outer diameter, protruding 100 μm from a flange) was fitted to the end of a dermojet spring-powered jet injector for successful rabbit eye IV injection. Although this injector is promising evidence that non-damaging JI into the vitreous is possible, this device will likely suffer from many of the same disadvantages as conventional needle injection due to the use of a microneedle to pierce the sclera.

On the contrary, a cost-effective IV JI system that delivers concentrated drug to a targeted region of the vitreous with a lowered risk of accidental needle wounds and infection would transform eye care. This study asserts the feasibility of adapting existing Lorentz-force actuated JI technology to IV injections, one step towards this transformation.

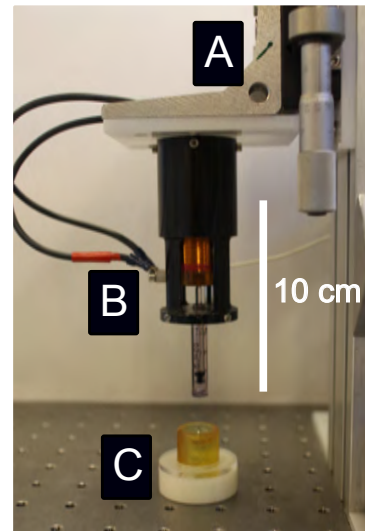


Fig. 1. IV jet injector. (A) Injector height adjustment stage. (B) Lorentz-force actuated jet injector. (C) 3D-printed artificial orbit for eye mechanical support and positioning.

II. MATERIALS & METHODS

A. Injector Hardware

The hardware component of the system was similar to a previously described MIT BioInstrumentation Lab jet injector [6]. The injection jet orifice was 221 μm in diameter, and the ampoule diameter was such that a 1 mm plunger stroke displaced 10 μL of fluid. A pair of power amplifiers (AE Techron 7224, Elkhart, IN) arranged in a bridged

*This work was supported by Sanofi S.A., Paris, France

¹J. E. White is with the Department of Mechanical Engineering, Massachusetts Institute of Technology, Room 3-147, 77 Massachusetts Ave, Cambridge, MA 02139, USA phone: 830-279-7380 e-mail: jamesw at mit.edu

²J. H. Chang are with the Department of Mechanical Engineering, Massachusetts Institute of Technology, Room 3-147, 77 Massachusetts Ave, Cambridge, MA 02139, USA

³N. C. Hogan is with the Department of Mechanical Engineering, Massachusetts Institute of Technology, Room 3-147, 77 Massachusetts Ave, Cambridge, MA 02139, USA

⁴I. W. Hunter is with the Department of Mechanical Engineering, Massachusetts Institute of Technology, Room 3-154, 77 Massachusetts Ave, Cambridge, MA 02139, USA

configuration were used to supply power to the coil. A real-time programmable automation controller (PAC) (National Instruments cRIO-9024, Austin, TX) was used for device control, camera triggering, and user input. The jet injector was fixed to an adjustable vertical linear stage, decoupling human injection error from the trials.

Several new components were added to the system to facilitate analysis of delivery to the eye. Because *ex vivo* eyes were used, a stage was designed and 3D printed to act as the load-bearing hemisphere of the orbit during injection, holding an eye fixed in the desired orientation. A control panel and amplifier interface were also developed for the IV JI system. A high-speed camera (Vision Research Phantom v9, Wayne, NJ) was mounted facing perpendicular to the path of injection. A photo of the eye injection environment is shown in Fig. 1.

B. Velocity Bang-PD Controller

The controller used in an earlier version of the jet injector was replaced to facilitate IV JI. The speed and duration of an injection jet are key factors in the resulting penetration depth [7], which is essential to control in an IV injection. In an IV JI, the jet speed must be high enough to pierce the sclera [9], yet the jet duration must be short enough that it does not damage the retina. To estimate the coil velocity, a discrete derivative of the 100 kHz-sampled coil position was smoothed by a 10 kHz Butterworth low-pass filter.

In the control scheme, an initial bang controller (upper limit of a bang-bang controller) is used to reach a high coil velocity in minimum time. This stage is followed by PD velocity control to a preset follow-through velocity. Within 5% of the preset coil position (proportional to injection volume), the controller transitions into PD position control. The controller can be represented by the block diagram in Fig. 2.

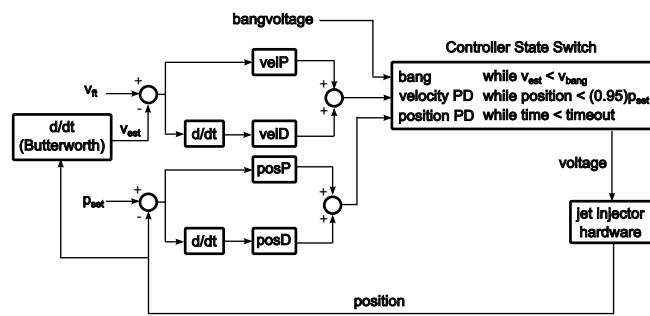


Fig. 2. Block diagram of control algorithm. The controller state switch progresses to the next state when the ‘while’ condition is false. v_{est} is the real-time estimated velocity, v_{bang} is the set bang controller velocity, $voltage$ is the voltage command to the amplifier, $bangvoltage$ is a bang control parameter, $position$ is the position measured by the potentiometer, v_{ft} is the set follow-through velocity, p_{set} is the set injection position, $velP$, $velD$, $posP$, $posD$ are control parameters, $time$ increases throughout the injection, and $timeout$ is a preset injection time limit.

C. Injection Protocol

Nine rabbit eyes were obtained through the MIT Tissue Harvest Program using procedures approved by the MIT

Committee on Animal Care and in accordance with the NIH Guide for the Use and Care of Laboratory Animals. Explanted eyes were refrigerated in saline solution for no more than 4 hours before the injection trial. In each trial, the ampoule nozzle was placed in light contact with the sclera at 3 mm from the *limbus corneae*, the recommended site for human IV injection [10]. Then, 40 μ L of 0.25% bromophenol blue dye solution was injected in the direction of the optic nerve area. Bang controller set peak coil velocities ranged from 2.04 m/s to 2.42 m/s and set follow-through velocities ranged from 0.05 m/s to 0.20 m/s.

Immediately after injection, eyes were embedded in optimal cutting temperature compound (Tissue-Tek O.C.T. Compound 4583, Torrance, CA) in liquid nitrogen. The samples were wrapped in foil and stored at -20°C until needed. The resulting O.C.T.-eye blocks were sectioned and imaged in 30 μ m increments superior and perpendicular to the axis of injection using a cryostat vibratome (GMI Inc. Vibratome UltraPro 5000, Ramsey, MN).

III. RESULTS

Although the controller set-points were based on coil position and velocity, it is useful to estimate the velocity of the fluid jet. Average jet velocities calculated volumetrically from coil speed agreed well with high-speed camera estimation of jet velocity during the follow-through phase of the controller. However, during the bang phase of the controller, the system dynamics resulted in a large error between camera-measured and volumetric-estimated jet speed. To estimate peak jet velocities in spite of these dynamics, we solved for jet velocity using Bernoulli’s principle,

$$v = \sqrt{\frac{2P}{\rho}}, \quad (1)$$

where v is the average peak jet velocity, ρ is the density of the fluid, and P is the pressure in the ampoule. To estimate the pressure in the ampoule, we calculated the force on the piston tip and divided by ampoule area. Force was estimated by subtracting the force used to accelerate the coil system from the Lorentz force generated by the coil.

$$P = (KI - ma)/A, \quad (2)$$

where K is the motor constant, I is the peak current passing through the coil, m is the mass of the coil system, a is the acceleration of the coil system, and A is the area of the piston. The acceleration of the coil system was estimated using the rise time (t_{rise}) and peak coil velocity (v_{peak}) as follows:

$$a = v_{peak}/t_{rise}. \quad (3)$$

A. Velocity Bang-PD Controller

The controller improved the velocity profile for low-duration II. From rest, the bang controller reached coil velocities of 2.5 m/s within 1.5 ms, and the PD velocity controller slowed the coil to the follow-through velocity within 1 ms, shown in Fig. 3. The high-velocity segment of the injection lasted less than 2 ms, about half the duration of the earlier controller's high-velocity jet. The PD position controller activated when the position was within 5% of the set-point. The controller held the set-point until the injection time was reached.

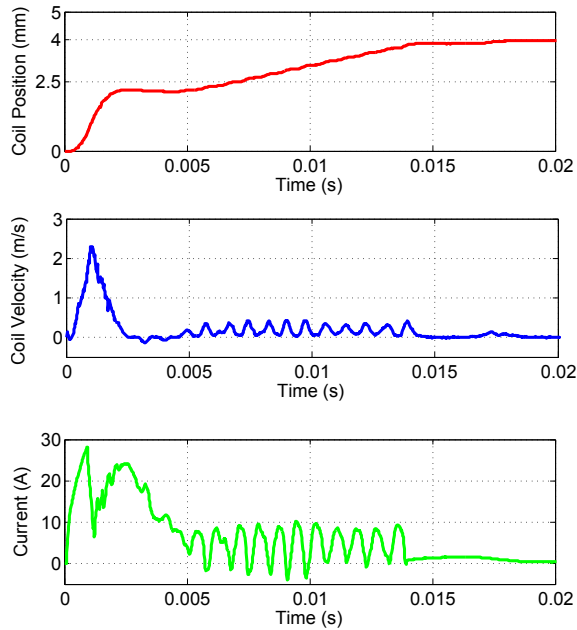


Fig. 3. Representative injection results with bang-PD velocity controller. Set parameters: 2.5 m/s coil bang velocity; 0.2 m/s coil follow velocity; 40 μ L delivery volume (4 mm set-point).

Bang control of the injector system overshoot the target velocity, as shown in Fig. 3, due to the controller lag and third-order Lorentz-force actuator system dynamics. When switching to the follow-through velocity segment, the PD controller undershot the set velocity, even reversing direction. Tuning the PD controller to undershoot ensured that fall time was short, which is critical to minimize tissue destruction, and the real jet velocity never dropped below zero (verified by high-speed camera). The overshoot and undershoot were not repeatable, due to the time-varying dynamics of the system (i.e., ampoule degradation) and variation in eye tissue (i.e., scleral thickness and intraocular pressure). At low velocities the system exhibited periodic oscillations, possibly due to non-linear friction of the ampoule.

B. Ex Vivo Rabbit Intravitreal Injections

A typical injection time-line is shown in Fig. 4. No vitreal reflux was observed after any injection, but dye accumulation at the injection site has not yet been quantified. Sectioning revealed that 7 out of 9 eyes exhibited retinal tearing. To numerically characterize the post-injection eye results, two

metrics were defined: retinal tear diameter and entry hole diameter. These metrics were measured as shown in Fig. 5. Two injections resulted in no retinal tearing, as shown in Fig. 6, and had peak jet velocities of less than 171 m/s and follow-through velocities of less than 6.8 m/s.

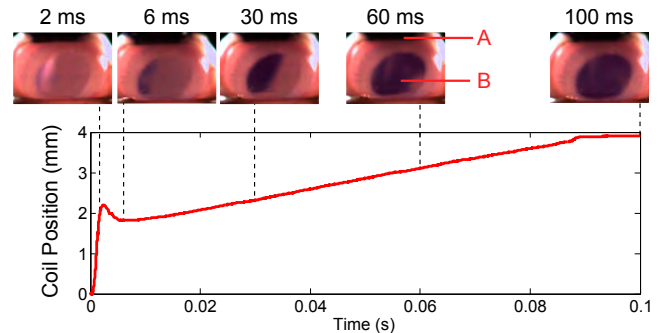


Fig. 4. Time-line of injection, showing high-speed camera images and velocity profile. (A) Injection site. (B) Target site. Peak jet velocity: 170 m/s; average follow-through velocity: 6.7 m/s. Eye exhibited no retinal tearing.

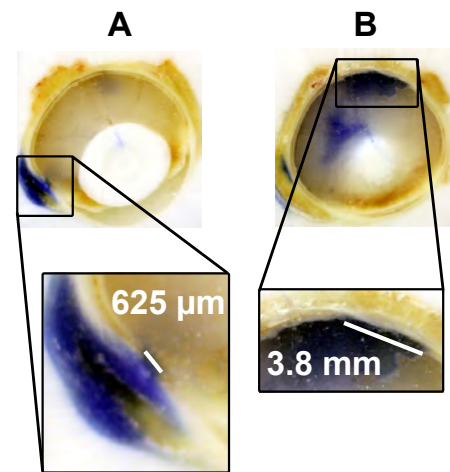


Fig. 5. Injection result measurement methodology. (A) Entry hole (marked by box) diameter is measured as the largest width of choroid puncture in sections. (B) Retinal tear (marked by box) diameter is measured as the largest width of detached retina in sections.

To relate velocity profile characteristics to eye damage metrics, the peak velocity and average follow-through velocity of each injection were recorded. Next, to isolate the effects of each velocity, two groups were formed: five injections with similar peak velocities ($161 \text{ m/s} \pm 8 \text{ m/s}$) and four injections with similar follow-through velocities ($6.45 \text{ m/s} \pm 0.41 \text{ m/s}$). Remaining eye injection results were not used for analysis. For each isolation group, the jet velocities were plotted against both eye damage metrics, shown in Fig. 7. Although more trials are required to show significance, plots suggest a positive correlation between tissue damage and increasing velocities, and also reveal velocity thresholds at which retinal tearing begins. A follow-through jet velocity threshold may exist between 6.58 m/s and 28.9 m/s, and a peak velocity threshold may exist between 170 m/s and 201 m/s.

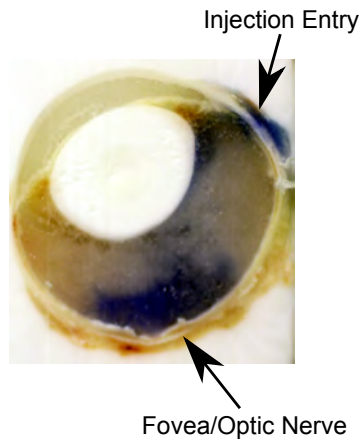


Fig. 6. IV JI exhibiting no post-injection damage. (Superior view of cross-section, showing injection site and target.)

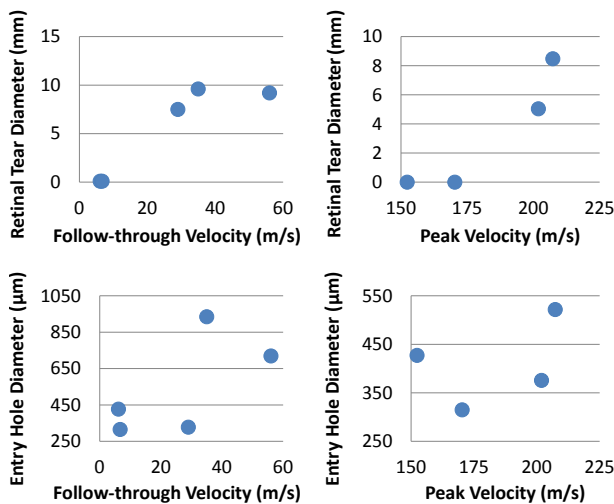


Fig. 7. Plots of two velocity profile characteristics vs. two eye damage metrics. For varying follow-through velocities, the peak velocity is $161 \text{ m/s} \pm 8 \text{ m/s}$; for varying peak velocities, the follow-through velocity is $6.45 \text{ m/s} \pm 0.41 \text{ m/s}$.

IV. DISCUSSION

IV JI can be accomplished using a pre-existing linear Lorentz-force actuated jet injector with the addition of a bang-PD velocity controller. Although a greater number of *ex vivo* and *in vivo* trials must be run to soundly characterize the system behavior, the current data provides us with some insight. Fig. 7 suggests that low peak and follow-through velocities prevent retinal tearing. Entry hole diameter may be positively correlated with both velocities, albeit with more deviation. Four eyes had entry hole diameters less than $400 \mu\text{m}$, within the range of needle sizes commonly used in IV injections. This is important, as pain and drug reflux have been shown to increase with larger needles [11] and may similarly increase with larger IV JI entry holes. Moreover, the IV JI duration is less than 100 ms, minimizing patient discomfort and procedure time.

Eye sections with and without retinal tearing suggest that injections can target the optic nerve, as shown by the dye

concentration in Fig. 6. In a needle injection, delivery to this area relies on convection and diffusion, and much of the drug is transported elsewhere. Higher concentrations of drug near the target site are favorable because they reduce the total amount of drug needed and the systemic impact of treatment [12].

Future work will focus on improving controller performance, post-injection analysis, and mechanical design. This study suggests that more repeatable controller performance will lead to more repeatable injections without retinal tearing. Analysis improvements include further characterization of the velocity waveform and quantification of volume delivered to target. Mechanically, redesigning the ampoule nozzle geometry may decrease damage to the eye by reducing the divergence and diameter of the exit stream. Finally, dynamics of the injection system, such as piston tip compliance and ampoule strain, may be simplified mechanically or compensated for with a redesigned control or sensing scheme.

ACKNOWLEDGMENT

The authors would like to thank members of the BioInstrumentation Lab for their advice with the development of the IV JI system. The authors would especially like to thank Bryan Ruddy for contributions to jet velocity estimation.

REFERENCES

- [1] P. V. Algvere, B. Sten, S. Seregard, and A. Kvanta, "A prospective study on intravitreal bevacizumab (avastin) for neovascular age-related macular degeneration of different durations," *Acta Ophthalmologica*, vol. 86, pp. 482–489, Aug. 2008.
- [2] J. O. Mason, P. A. Nixon, and M. F. White, "Intravitreal injection of bevacizumab (avastin) as adjunctive treatment of proliferative diabetic retinopathy," *American Journal of Ophthalmology*, vol. 142, no. 4, pp. 685–688, 2006.
- [3] G. Sunaric-Mgevand and C. J. Pournaras, "Current approach to postoperative endophthalmitis," *The British journal of ophthalmology*, vol. 81, no. 11, pp. 1006–1015, 1997.
- [4] C. Shima, H. Sakaguchi, F. Gomi, M. Kamei, Y. Ikuno, Y. Oshima, M. Sawa, M. Tsujikawa, S. Kusaka, and Y. Tano, "Complications in patients after intravitreal injection of bevacizumab," *Acta Ophthalmologica*, vol. 86, no. 4, pp. 372–376, 2008.
- [5] P. Y. S. Chua, I. Mitrut, A.-M. Armbrecht, A. Vani, T. Aslam, and B. Dhillon, "Evaluating patient discomfort, anxiety, and fear before and after ranibizumab intravitreal injection for wet age-related macular degeneration," *Archives of Ophthalmology*, vol. 127, pp. 313–316, July 2009.
- [6] B. Hemond, "A lorentz-force actuated controllable needle-free drug delivery system," Master's thesis, Massachusetts Institute of Technology, Cambridge, Massachusetts, Feb. 2006.
- [7] A. Taberner, N. C. Hogan, and I. W. Hunter, "Needle-free jet injection using real-time controlled linear lorentz-force actuators," *Medical Engineering & Physics*, 2012.
- [8] G. A. Peyman, K. Hosseini, and M. Cormier, "A minimally invasive jet injector for intravitreal and subconjunctival injection," *Ophthalmic Surgery, Lasers & Imaging*, vol. 43, pp. 57–62, January/February 2012.
- [9] J. S. Pulido, M. E. Zobitz, and K.-N. An, "Scleral penetration force requirements for commonly used intravitreal needles," *Eye*, vol. 21, pp. 1210–1211, 2007.
- [10] J. F. Korobelnik, M. Weber, S. Y. Cohen, and E. Panel, "Guidelines for intravitreal injections," *Journal francais d'ophtalmologie*, vol. 32, pp. e1–e2, 2009.
- [11] J. S. Pulido, C. M. Pulido, S. J. Bakri, C. A. McCannel, and J. D. Cameron, "The use of 31-gauge needles and syringes for intraocular injections," *Eye*, vol. 21, pp. 829–830, 2007.
- [12] S. Ding, "Recent developments in ophthalmic drug delivery," *Pharmaceutical Science & Technology Today*, vol. 1, no. 8, pp. 328 – 335, 1998.